

MULTI-INSTRUMENT X-RAY OBSERVATIONS OF THERMONUCLEAR BURSTS WITH SHORT RECURRENCE TIMES

L. KEEK¹, D. K. GALLOWAY², J. J. M. IN 'T ZAND³, A. HEGER¹

Draft version August 21, 2018

Abstract

Type I X-ray bursts from low-mass X-ray binaries result from a thermonuclear runaway in the material accreted onto the neutron star. Although typical recurrence times are a few hours, consistent with theoretical ignition model predictions, there are also observations of bursts occurring as promptly as ten minutes or less after the previous event. We present a comprehensive assessment of this phenomenon using a catalog of 3387 bursts observed with the BeppoSAX/WFCs and RXTE/PCA X-ray instruments. This catalog contains 136 bursts with recurrence times of less than one hour, that come in multiples of up to four events, from 15 sources. Short recurrence times are not observed from so-called ultra-compact binaries, indicating that hydrogen burning processes play a crucial role. As far as the neutron star spin frequency is known, these sources all spin fast at over 500 Hz; the rotationally induced mixing may explain burst recurrence times of the order of 10 min. Short recurrence time bursts generally occur at all mass accretion rates where normal bursts are observed, but for individual sources the short recurrence times may be restricted to a smaller interval of accretion rate. The fraction of such bursts is roughly 30%. We also report the shortest known recurrence time of 3.8 minutes.

Subject headings: accretion, accretion disks — methods: observational — stars: neutron — X-rays: binaries — X-rays: bursts

1. INTRODUCTION

Type I X-ray bursts are thought to result from thermonuclear flashes of hydrogen and/or helium in the envelope of neutron stars (Woosley & Taam 1976; Maraschi & Cavaliere 1977; Lamb & Lamb 1978). This material is accreted through Roche-lobe overflow from a lower-mass companion star (low-mass X-ray binary, LMXB). Current one-dimensional models successfully explain burst features such as the peak flux, the fluence, decay time and recurrence time (e.g., Woosley et al. 2004; Heger et al. 2007; see Wallace & Woosley 1981; Fujimoto et al. 1981; Fushiki & Lamb 1987 for earlier work). During the flash, over 90% of the accreted hydrogen and helium is expected to burn to carbon and heavier elements (e.g., Woosley et al. 2004). For the next flash to occur, a fresh layer of hydrogen/helium must first be accreted. At typical accretion rates of up to approximately $10^{-8} M_{\odot} \text{yr}^{-1}$ this takes at least a few hours.

X-ray bursts have been observed since the 1970's (Grindlay et al. 1976; Belian et al. 1976) from approximately 90 sources in our Galaxy, with recurrence times of hours up to days (e.g., Lewin et al. 1993; Strohmayer & Bildsten 2006). Lewin et al. (1976) reported the detection with *SAS-3* of three bursts that were separated by only 17 and 4 minutes. These bursts originated from a crowded region and, therefore, source confusion cannot be ruled out. In the 1980's similar recurrence times as short as 10 minutes were observed from both 4U 1608-522 with *Hakucho* (Murakami et al. 1980) and from EXO 0748-676 with *EXOSAT* (Gottwald et al.

1986, 1987a). This rare phenomenon implies that hydrogen and helium is left over somewhere on the star after the initial flash, because the recurrence time is too short to accrete enough fuel for the subsequent burst(s). This is at odds with the current models, that predict an almost complete burning of the available hydrogen and helium on the entire star surface.

Boirin et al. (2007) analyzed 158 hours of *XMM-Newton* observations of EXO 0748-676, which revealed short recurrence time bursts in groups of two (doubles) and three (triples). This relatively large burst sample revealed that on average bursts with a short recurrence time (8 to 20 minutes) are less bright and energetic than bursts with 'normal' recurrence times (over 2 hours). The fit of a black body model to the burst spectrum shows a lower peak temperature, while the emitting area is the same. The profiles of short recurrence time bursts seemingly lack the long 50 s to 100 s tail caused by *rp*-process burning, which indicates that the burst fuel contains less hydrogen. After a double or triple it takes on average more time before another burst occurs, suggesting a more complete burning of the available fuel.

Galloway et al. (2008) showed that there are more sources that show this behavior, with bursts occurring in groups of up to four bursts, and with recurrence times as short 6.4 minutes. The short recurrence times were observed predominantly when the persistent flux is between approximately 2% and 4% of the Eddington limited flux. Furthermore, indications were found for the association of short recurrence times and the accretion of hydrogen-rich material. The shortest recurrence time previously reported is 5.4 minutes (Linares et al. 2009).

Different ideas have been put forward to explain this rare bursting behavior. As most of the models only resolve the neutron star envelope in the radial direction, it is possible that short recurrence time bursts are due to

laurens@physics.umn.edu

¹ School of Physics and Astronomy, University of Minnesota, 116 Church ST SE, Minneapolis, MN 55455, USA

² Center for Stellar and Planetary Astrophysics, Monash University, VIC 3800, Australia

³ SRON Netherlands Institute for Space Research, Sorbonnelaan 2, NL - 3584 CA Utrecht, The Netherlands

multi-dimensional effects, such as the confinement of accreted material on different parts of the surface, possibly as the result of a magnetic field (e.g., Melatos & Payne 2005; Lamb et al. 2009). Boirin et al. (2007), however, found that the different bursts originate from an emitting area of similar size. Furthermore, the indication of a different fuel composition for the bursts with short recurrence times, argues against any scenario where accreted material of the same composition burns on different parts of the surface.

The idea of a burning layer with an unburned layer on top has been investigated (Fujimoto et al. 1987). After the first layer flashes, the second layer could be mixed down to the depth where a thermonuclear runaway occurs. Mixing may be driven by rotational hydrodynamic instabilities (Fujimoto 1988) or by instabilities due to a rotationally induced magnetic field (Piro & Bildsten 2007; Keek et al. 2009). The mixing processes take place on the correct time scale of approximately ten minutes. Although this scenario is able to explain many of the observed aspects of short recurrence time bursts, it has not been reproduced with a multi-zone stellar evolution code that includes a full nuclear burning network. Taam et al. (1993) created models that exhibit ‘erratic’ bursting behavior, reminiscent of short recurrence time bursts. Later versions of the employed code, however, no longer produce this, most likely because of the inclusion of a more extensive nuclear network (Woosley et al. 2004). As a different explanation for the reignition, Boirin et al. (2007) suggested a waiting point in the chain of nuclear reactions. There may be a point in the chain where a decay reaction with a half life similar to the short recurrence times stalls nuclear burning before continuing.

We use an improved version of the burst catalog compiled by Galloway et al. (2008), that is extended with the X-ray burst observations of the WFCs on-board *BeppoSAX* (e.g., Cornelisse et al. 2003). This is the largest collection of X-ray bursts used in any study to date. This allows us to study the short recurrence time phenomenon in much more detail.

2. OBSERVATIONS AND ANALYSIS METHODS

2.1. Nomenclature

In this paper we name the different kinds of bursts using the conventions of Boirin et al. (2007). Bursts with recurrence (waiting) times shorter than one hour are referred to as *short waiting time (SWT)* bursts, while longer recurrence time bursts are *long waiting time (LWT)* bursts. The one-hour boundary is chosen to discriminate between the two distinct groups of bursts we observe (Sect. 3.5). A burst *event* is defined as a series of bursts, where any two or more subsequent bursts are separated by a short waiting time. We refer to an event with one, two, three, or four bursts as a *single*, *double*, *triple*, or *quadruple* burst, respectively. Furthermore, we call a double, triple, or quadruple burst a *multiple-burst event*. For the bursts within a multiple-burst event, we use the terms *first burst* and *follow-up burst*, where the former refers to the LWT burst and the latter to any SWT burst in the event.

2.2. Burst catalog

Because SWT bursts are rare, we need a large sample of bursts to study them well. We use a preliminary ver-

sion of the Multi-INstrument Burst ARchive (MINBAR), which is a collection of Type I bursts that are observed with different X-ray instruments, and that are all analyzed in a uniform way. MINBAR is a continuation of the effort which started with the *RXTE* PCA burst catalog by Galloway et al. (2008), combined with the many X-ray bursts observed with the WFCs on *BeppoSAX* (e.g., Cornelisse et al. 2003). The catalog will be presented in full in a forthcoming paper. Currently it contains information on 3402 bursts from 65 sources, among which are 136 SWT bursts (MINBAR version 0.4). In comparison, Galloway et al. (2008) report 1187 bursts from 48 sources, among which are 84 bursts with a short recurrence time, in that paper defined as < 30 min (MINBAR contains 110 SWT bursts using this criterion).

2.3. Instruments

The *Rossi X-ray Timing Explorer (RXTE)* was launched on December 30, 1995. One of the instruments on-board is the Proportional Counter Array (PCA; Jahoda et al. 2006), consisting of five proportional counter units (PCUs) which observe in the 1 to 60 keV energy range. The PCA has a large collecting area of 8000 cm² (1600 cm² for each PCU). The PCUs are co-aligned and have a collimator that gives a 1° FWHM field of view. As part of the primary mission objective of *RXTE*, the PCA gathered a large amount of exposure time on the galactic LMXB population. The observations we use have an average duration of 78 min. We use all data that was publicly available in July 2008 (compared to June 2007 for Galloway et al. 2008).

The High-Energy X-ray Timing Experiment (HEXTE; Gruber et al. 1996) on *RXTE* consists of two clusters of NaI/CsI scintillation detectors that allow for observations in the 15 to 250 keV energy range. If available, we combine PCA and HEXTE observations to obtain a broad band X-ray spectrum, when studying the persistent flux of bursting sources.

The All-Sky Monitor (ASM) on *RXTE* consists of three scanning shadow cameras (SSCs) on a rotating beam that image a large part of the sky each satellite orbit, in a series of short 90 s observations. The SSCs observe in the 1.5 to 12 keV energy range.

A few months after *RXTE*, the *BeppoSAX* observatory was launched in April 1996 (Boella et al. 1997), and it was operational until April 30, 2002. On-board were two Wide-Field Camera’s (WFCs) which faced in opposite directions (Jager et al. 1997). The WFCs were sensitive in the 2 to 28 keV band-pass and each camera imaged at any time 40° × 40° of the sky using a coded mask aperture. Bi-yearly observations of the Galactic Center were performed, resulting in a large exposure time for many of the LMXBs in the Galaxy (in 't Zand et al. 2004). the WFC observations have a mean duration of 255 min. We use all WFC data.

For the majority of the bursters, which are located near the Galactic Center, we gather a total net exposure time of approximately 50 days.

Both observatories were placed in a low Earth orbit of approximately 96 minutes. During the observation of a particular source, the source is obscured by the Earth for a typical duration of approximately 36 minutes per orbit. Furthermore, when the satellites passed through the South Atlantic Anomaly (SAA), the detectors were

turned off to prevent damage. This introduces data gaps of 13 to 26 minutes long. The precise length of the different data gaps depends on the latitude of the source with respect to the satellite orbit, which was different for *BeppoSAX* and *RXTE*.

2.4. Burst analysis

We briefly discuss the process of the burst analysis. The generation of data products for the different instruments is handled identically to the studies by Galloway et al. (2008) and Cornelisse et al. (2003). Our method of burst analysis is in principle the same as for those studies, but extra care was taken to ensure that results from different instruments are directly comparable. For more details of the analysis of PCA and WFC data, we refer to Galloway et al. (2008) and Cornelisse et al. (2003), respectively.

To find burst occurrences, we generate light curves for each instrument, for each known bursting source. In the light curves we locate all events that rise significantly above the background, e.g., exceeding the mean flux level by at least four times the standard deviation. These events are checked by eye for the characteristic profile of a fast rise and an exponential-like decay.

Next, time-resolved spectroscopy is performed on the candidate bursts. We divide the individual bursts in time intervals, such that we obtain for each interval a burst spectrum with similar and sufficient statistics. The net burst spectrum is obtained by subtracting the spectrum of the persistent emission observed during the entire observation, excluding the burst (e.g., Kuulkers et al. 2002). We fit the burst spectra with a black body model, taking into account the effects of interstellar absorption (Morrison & McCammon 1983; solar abundances from Anders & Ebihara 1982). From this we find a black body temperature and radius, as well as the unabsorbed flux. By extrapolating the fitted black body model beyond the observed energy range, we obtain the bolometric unabsorbed flux. Integrating the flux over the burst yields the burst fluence.

The decay time is determined by fits to the burst light curve. We obtain the net burst light curve by subtracting the persistent flux, as measured in the entire observation, excluding the burst. We start fitting the decay when the flux drops below 90% of the peak flux. This has the advantage that we are less sensitive to the Poisson noise at the peak or to the effects of radius expansion. The decay of many bursts is fit well by two exponentials, with two exponential decay times. For some bursts two exponentials did not yield a statistically better fit than a single exponential. For those bursts we report only a single decay time. It should be noted that not for all bursts a good fit was obtained, but the ‘best’ fit still provides a qualitative description of the burst decay.

The determination of the burst decay time is currently not done uniformly for the different instruments. For the PCA the bolometric flux is used, while for the WFCs the flux in counts per second is used. We compared the decay times obtained for 15 bursts that have been observed by both instruments. On average, the decay times for the WFC bursts are $(22 \pm 7)\%$ longer than for the PCA bursts. Although the decay time scales are not fully compatible across the different instruments, we can still use them to differentiate between short bursts and the longer

bursts with the *rp*-process tail.

2.5. Persistent emission and mass accretion rate

We obtain the persistent flux for each burst by fitting the spectrum from the entire observation, excluding the burst. By extending the fitted spectral model (typically a comptonized spectrum or a black body + power law; see Galloway et al. 2008 for details) outside the observed energy range, we determine the bolometric correction. The uncertainty in the bolometric correction can be as small as 10%, when we combine *RXTE* PCA and HEXTE observations to obtain a broadband spectrum. The *BeppoSAX* WFCs, however, do not have such broad energy coverage, and some PCA observations suffer from source confusion, which leads to an increased uncertainty in the bolometric correction of up to 30%.

To convert flux to luminosity and fluence to energy, we multiply by $4\pi d^2$, with d the distance to the source. We use the distances from Kuulkers et al. (2003) for globular cluster sources, and from Galloway et al. (2008) (distances from photospheric-radius expansion bursts observed with the PCA) and Liu et al. (2007) for the other sources. Most measurements of the distance have an uncertainty of the order of 30%. Combined with a 30% error in the bolometric correction, this leads to an uncertainty in the luminosity and the fluence of up to approximately 70%.

The persistent X-ray emission from an LMXB mainly originates from the inner part of the accretion disk, and, therefore, is a measure of the mass accretion rate (e.g., Galloway et al. 2004b). We express the mass accretion rate \dot{M} in terms of the Eddington limited accretion rate \dot{M}_{Edd} by equating their ratio to the ratio of the persistent luminosity L and the Eddington luminosity for hydrogen accreting sources $L_{\text{Edd}} = 2 \cdot 10^{38} \text{ erg s}^{-1}$: $\dot{M}/\dot{M}_{\text{Edd}} = L/L_{\text{Edd}}$. L_{Edd} depends on the neutron star mass and the hydrogen fraction of the accreted material (e.g., Bildsten 1998), both of which are not known to great precision for most LMXBs. The current observational constraints on the mass (Lattimer & Prakash 2007) introduce an uncertainty of several tens of percents. Furthermore, we assume that the accretion process has an efficiency of 100%. It is possible that part of the matter leaves the system in a jet, such as observed in black-hole binaries (e.g., Fender et al. 2005). In this paper, however, we neglect this possibility and assume the luminosity is a good measure of the mass accretion rate. We also neglect any anisotropy factors that may arise from the inclination of the disk with respect to the line of sight; because the inclination is ill-constrained for most LMXBs, we assume isotropic emission.

The combined uncertainties are quite large, but this only plays a role when we compare different sources. It is, however, of no consequence when we compare the bursts of any single source. We will still compare different sources, but one must be careful to keep these uncertainties in mind.

3. RESULTS

3.1. Source selection

The MINBAR catalog contains X-ray bursts from 65 sources, 15 of which exhibit SWT bursts (Table 1), i.e., bursts with a recurrence time shorter than one

TABLE 1
OVERVIEW OF 15 BURSTERS WITH SHORT RECURRENCE TIMES.

Name	ν_{spin} (Hz)	t_{exposure} (days)	MINBAR bursts	Single	Double	Triple	Qua- druple	Remarks
EXO 0748-676	552 ^a	83.1	269	251	9	0		Triples: Boirin et al. (2007); Appendix
GS 0836-429		30.9	17	17	0			Double: Aoki et al. (1992)
4U 1323-62		53.9	41	33	4			
4U 1608-522	620 ^b	52.4	67	60	2	1		
4U 1636-536	581 ^c	60.6	241	212	11	1	1	
MXB 1658-298	567 ^d	49.8	27	25	1			
4U 1705-44		60.1	125	108	5	1	1	
XTE J1710-281		47.9	18	16	1			
4U 1735-44		54.7	50	38	6			
2S 1742-294		56.3	269	240	10	3		
EXO 1745-248 (Tz 5) ^f		48.3	24	15	1	1	1	Type II bursts? (Galloway et al. 2008)
4U 1746-37 (NGC 6641) ^f		55.1	31	15	8			Two sources? (Galloway et al. 2004a)
SAX J1747.0-2853		71.5	63	57	3			
Aql X-1	549 ^e	34.3	60	49	4	1		
Cyg X-2 ^f		55.7	55	45	5			

^a Galloway et al. (2009)

^b Muno et al. (2002)

^c Strohmayer et al. (1998)

^d Wijnands et al. (2001)

^e Zhang et al. (1998)

^f Source excluded from our analysis. See Sect. 3.1 for details.

hour. We exclude the Rapid Burster, which is known to exhibit Type II bursts, which are not of thermonuclear origin (e.g., Lewin et al. 1993). Interestingly, no multiple-burst events are detected from candidate and confirmed ultra-compact binaries (UCXBs). The companion star in a UCXB is thought to be an evolved star, donating hydrogen-poor matter to the neutron star (in 't Zand et al. 2005). For confirmed UCXBs the binary period has been measured, while candidates are identified by tentative measurements of the period, by a low optical to X-ray flux, or by stable mass transfer at rates below 1% of the Eddington limited rate. We employ the list of (candidate) UCXBs from in 't Zand et al. (2007), which omits candidates proposed on the basis of their X-ray spectrum, which is likely a less reliable method. From these sources we find 229 bursts, none of which are SWT bursts. The frequent burster 4U 1728-34 (GX 354-0) is suspected of being a UCXB based on its bursting behavior (Galloway et al. 2008). 543 bursts of this source are present in MINBAR, but no multiple-burst events. As this strongly suggests that SWT bursts are limited to hydrogen-rich accretors, we exclude in our studies the list of (candidate) UCXBs from in 't Zand et al. (2007), with the addition of 4U 1728-34.

GX 17+2 and Cyg X-2 exhibit bursts at accretion rates close to the Eddington limit (e.g., Kuulkers et al. 2002), while most LMXBs do not show bursts above approximately 10% of Eddington (e.g., van Paradijs et al. 1988; Cornelisse et al. 2003). Of these two sources, Cyg X-2 exhibits SWT bursts. Due to the high accretion rate, however, the amount of matter accreted in between the bursts is enough to account for the amount of fuel burned in the bursts. Furthermore, Galloway et al. (2008) find indications that (some of) the bursts of GX 17+2 and Cyg X-2 could be Type II bursts. For these reasons we exclude these two sources as well.

The bursts from EXO 1745-248, located in the globular cluster Terzan 5, exhibit only weak evidence for cooling, which means that their thermonuclear origin is not firmly

established, and that they possibly are Type II bursts. Another sign that the bursting behavior is anomalous, is the fact that most sources in Table 1 exhibit more double bursts than triples and quadruples, while EXO 1745-248 has one of each. We exclude the source in our studies.

4U 1746-37, located in the globular cluster NGC 6641, exhibits both faint and bright bursts. Galloway et al. (2004a) found in PCA observations that the faint bursts occur at very regular intervals, unaffected by the occurrence of bright bursts, and vice versa. This lead to the speculation that the faint bursts originate from a different LMXB that is also located in NGC 6641. We, therefore, exclude the bursts from this source.

After excluding the mentioned sources, we consider 44 hydrogen-rich accretors from which we observe 2274 single, 56 double, 7 triple, and 2 quadruple events.

3.2. Source confusion

While the WFCs are imaging instruments, the PCA is not. The PCA's collimators restrict the field of view to 1° FWHM. Especially in crowded regions, such as near the Galactic Center, multiple X-ray sources may be in the field of view. For the sources in Table 1 we check the *RXTE* ASM light curves for any nearby bright X-ray sources that were active at the time of PCA burst observations. This is the case for 2S 1742-294 and SAX J1747.0-2853. Those bursts, for which we cannot reliably measure the persistent flux, are excluded from our studies.

The problem is small for SAX J1747.0-2853, because most of its bursts were observed with the WFCs, and we have a reliable measurement of the persistent flux for all three SWT bursts. For 2S 1742-294 the problem of source confusion plays a role for 61 bursts, including 12 out of 16 SWT bursts. Most of these bursts, including all SWT bursts, occur in the time interval MJD 52175–52195. The persistent flux as measured with the WFCs for bursts from that period varies by less than 10%. We assign the mean WFC persistent flux to those PCA bursts.

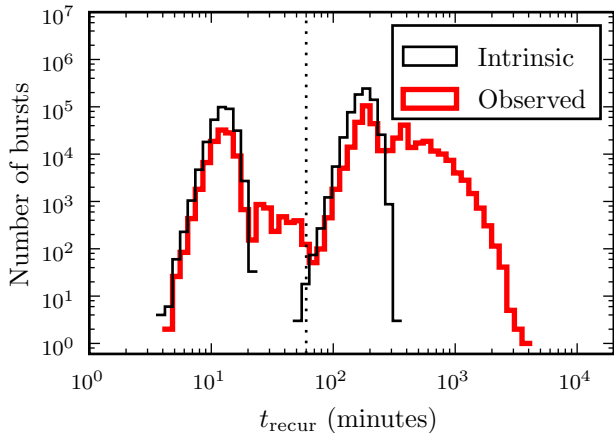


FIG. 1.— Histogram of simulated recurrence times t_{recur} . The *intrinsic* distribution is from a Monte Carlo simulation of 10^6 bursts with SWT and LWT recurrence times as well as SWT fraction from EXO 0748-676 (Boirin et al. 2007). The *observed* distribution includes the effect of data gaps due to Earth occultation and the South-Atlantic Anomaly. All bursts with $t_{\text{recur}} < 60$ min. (dotted line) are considered SWT bursts.

3.3. Data gaps and recurrence time

We define the recurrence time as the time since the previous burst from the same source in the catalog. Due to the frequent data gaps (Sect. 2.3), we must keep in mind that these are upper limits. Performing Monte Carlo simulations, we investigate the effect of the data gaps on the number of observed SWT and LWT bursts.

We generate a series of 10^6 burst occurrence times and check which bursts fall in data gaps. We use EXO 0748-676 as a template: we generate LWT and SWT bursts with an SWT fraction of 30%; we use the mean LWT and SWT recurrence times 3.0 hours and 12.7 minutes, respectively (Boirin et al. 2007); we position the bursts in time following a Gaussian distribution around the LWT or SWT t_{recur} , with a width of 16% of either t_{recur} (mean variability in persistent flux of a series of persistent sources; Keek et al. 2006) to model variations in the mass accretion rate. To check which of these bursts would be observed in the presence of data gaps, we assume a 96 min. satellite orbit, containing a 36 min. data gap due to Earth occultation. The presence and duration of data gaps due to the South-Atlantic Anomaly (SAA) depends on the position of the source and the satellite at the time of the observation. We model SAA data gaps by placing a 20 min. gap at a random phase of each orbit.

Only 49% of the generated bursts is ‘observed’, the rest coincide with a data gap. When a burst is missed, the recurrence time of the next burst, as seen from the previously detected burst, is incorrectly found to be longer: in the distribution of observed recurrence times a long tail of bursts is present at longer t_{recur} than present in the original distribution (Fig. 1). There are also bursts in between the Gaussian peaks of SWT and LWT bursts, but their number is less than 10% of the total number of SWT bursts. Because most of these bursts have $t_{\text{recur}} < 60$ min., we still consider them SWT bursts.

The fraction of bursts that are SWT bursts, is reduced when one or more bursts in a multiple-burst event occur during a data gap. While we start our simulations with an SWT fraction of 30%, the observed distribution has a fraction of 20%. We repeat the simulations with different

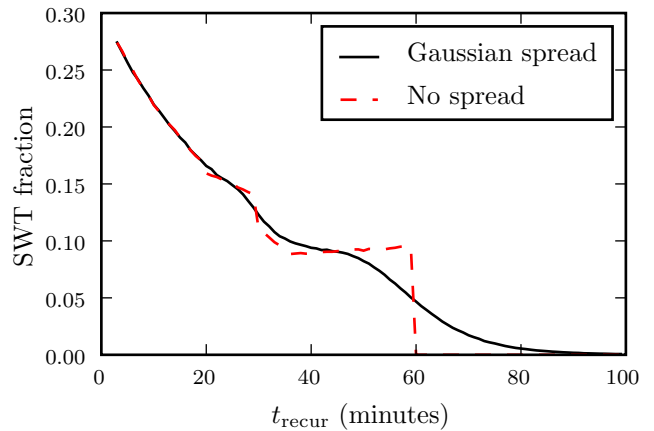


FIG. 2.— SWT fraction as a function of the SWT recurrence time t_{recur} . The solid line allows for variation of t_{recur} following a Gaussian distribution, while the dashed line does not. The latter drops to 0 at $t_{\text{recur}} = 60$ min., which is the largest SWT t_{recur} we consider.

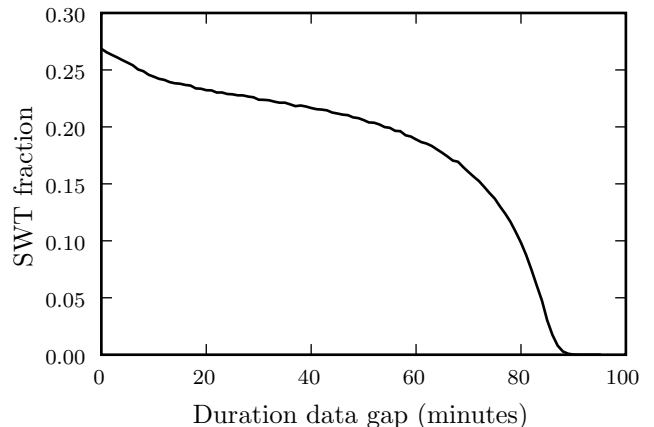


FIG. 3.— SWT fraction as a function of the duration of the Earth-occultation data gaps. The SWT fraction drops to 0 when the data gaps approach the 96 min. duration of the satellite orbit.

values of the SWT t_{recur} . The total fraction of detected bursts remains the same, but the SWT fraction drops from 30% to 10% for increasing t_{recur} , until t_{recur} exceeds the duration of the Earth occultation data gap (Fig. 2).

Repeating the simulations with different durations of the Earth-occultation data gap, the SWT fraction drops by only a few percent for longer data gaps, until the fraction quickly goes to 0, when an SWT recurrence time no longer fits in the observed part of the orbit (Fig. 3).

A similar decrease of the SWT fraction is expected if the duration of the observation is less than the SWT recurrence time. While the average exposure times of both the PCA and the WFCs exceed one hour, a substantial part of the observations had a shorter recurrence time: 19% of the WFC exposures and 66% of the PCA exposures were shorter than one hour.

3.4. Detection limits

The instruments we use have different detection limits. The WFCs had a substantially larger field of view than the PCA, which results in a higher background level. Furthermore, the PCA has a 46 times larger collecting area than each WFC. Consequently, we are able to find fainter bursts in PCA data than in WFC data (Fig. 4).

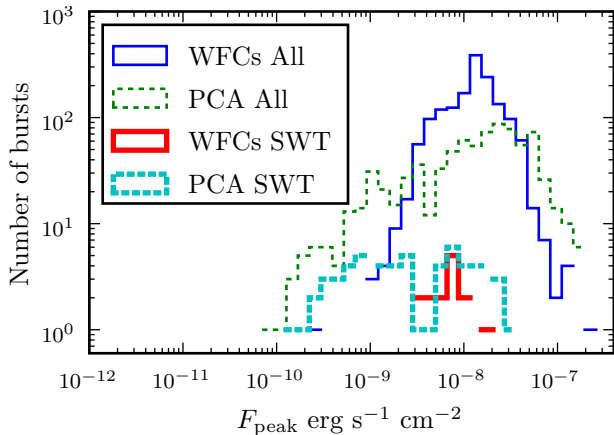


FIG. 4.— Histogram of observed peak burst flux F_{peak} for the WFCs and the PCA. Additionally we show the distributions for the short recurrence time bursts.

This is especially important for the SWT bursts, as they have been found to be on average fainter than the LWT bursts (e.g., Boirin et al. 2007). In the PCA data we find SWT bursts with peak flux F_{peak} as low as $1.6 \cdot 10^{-10} \text{ erg cm}^{-2} \text{ s}^{-1}$, while in the WFC data the faintest SWT burst has $F_{\text{peak}} = 3.6 \cdot 10^{-9} \text{ erg cm}^{-2} \text{ s}^{-1}$. As a result, we find many more SWT bursts with the PCA: for the PCA we find 76 SWT bursts out of a total of 910 bursts, and for the WFCs we find 14 SWT bursts out of 1560 bursts.

3.5. Recurrence times

We plot for all bursts the recurrence time t_{recur} as a function of the persistent luminosity L_{pers} (Fig. 5). While most bursts have a recurrence time of at least several hours, there is also a group of SWT bursts with $t_{\text{recur}} < 1$ hour. There is an intrinsic spread in t_{recur} due to, for example, variations in the mass accretion rate, or variations in the temperature in the neutron star envelope. We investigate whether the short recurrence times can be explained as the tail of the distribution of the long recurrence times. For this distribution we assume a Gaussian, even though it is not certain whether this is correct far from the mean. The data gaps modify the observed distribution, especially towards longer t_{recur} (Sect. 3.3). The leading part of the Gaussian, however, is not modified substantially, apart from the overall lower number of observed bursts due to the lower net exposure time (Fig. 1). We fit a Gaussian to the distribution of recurrence times between 1 and 3 hours with the center fixed at 3 hours. Extrapolating the best fit towards shorter t_{recur} , we predict 5.6 SWT bursts. The Poisson probability for the observed number of SWT bursts of 76, is negligibly small ($P \lesssim 10^{-10}$). Therefore, the short recurrence times follow a separate distribution.

There is a separation between bursts with short ($\lesssim 0.5$ hour) and long ($\gtrsim 1$ hour) recurrence times. Above $L_{\text{pers}} \gtrsim 6 \cdot 10^{36} \text{ erg s}^{-1}$, however, there are some bursts that have recurrence times of 30 to 60 minutes. Comparing the recurrence time distributions of SWT bursts ($t_{\text{recur}} < 1$ hour) at persistent luminosities below and above $L_{\text{pers}} = 6 \cdot 10^{36} \text{ erg s}^{-1}$, a KS-test yields $P = 0.16$, which means we can exclude at 84% that both distributions are the same. This is not a strong constraint, mainly due to the small number of bursts

with $L_{\text{pers}} < 6 \cdot 10^{36} \text{ erg s}^{-1}$. It is, however, consistent with the behavior of EXO 0748-676 during EXOSAT, XMM-Newton, and Chandra observations, that resulted in relatively large data sets, where SWT bursts with recurrence times exceeding 30 minutes only occurred when the persistent flux was larger (Gold 1968; Gottwald et al. 1987b; Boirin et al. 2007; Appendix).

There are SWT bursts at all values of L_{pers} where LWT bursts are observed, with the possible exception of $L_{\text{pers}} \gtrsim 3 \cdot 10^{37} \text{ erg s}^{-1}$, although this may be a statistical effect due to the lower number of bursts.

The α -parameter is defined as the ratio of the persistent fluence between bursts and the burst fluence. Assuming a burst fluence of $2.2 \cdot 10^{39} \text{ erg}$ — the average fluence of MINBAR single bursts from hydrogen-rich accretors — we draw lines of constant α ; $\alpha \simeq 40$ is a typical value for many bursters, while $\alpha \simeq 1000$ is observed for superbursters (e.g., in 't Zand et al. 2003). The effective α -value for the SWT bursts is far below $\alpha = 40$, which is the expected value for thermonuclear ignition of mixed hydrogen/helium fuel, highlighting the requirement for ignition of unburned fuel left-over from the previous burst.

We find the shortest recurrence time reported so-far⁴: 3.8 minutes for a double burst from 4U 1705-44, detected with the WFCs at MJD 51233.89.

3.6. Accretion rate dependence

We use the persistent luminosity L_{pers} as a measure of the mass accretion rate (Sect. 2.5). A Kolmogorov-Smirnov (KS) test finds that the distributions of all SWT and LWT as a function of L_{pers} are compatible ($P = 0.10$; Fig. 6): there are multiple-burst events at all mass accretion rates where normal bursts occur. This does not hold, however, for all individual sources. We investigate a few frequent bursters more closely. For EXO 0748-676 the distributions of single and multiple bursts are compatible ($P = 0.73$); 4U 1636-53 and 2S 1742-294 exhibit multiple bursts only in a small L_{pers} interval, while single bursts occur in a wider range of L_{pers} . The small L_{pers} intervals for these two sources do not seem to coincide. The uncertainty in the luminosity, however, is large (Sect. 2.5), so the intervals may still be consistent.

We find SWT bursts for only 15 out of 44 hydrogen-rich accretors. For most of the sources we can attribute the lack of SWT bursts to the low number of bursts detected per source. There are, however, two bursters, KS 1731-260 and GS 1826-24, from which we have detected over 300 LWT bursts per source, but no SWT bursts.

The position in so-called color-color diagrams, S_z , is regarded as a tracer of the mass accretion rate (Hasinger & van der Klis 1989). We compared the distribution of S_z for LWT and SWT bursts observed with the PCA from eight sources for which S_z is well defined: 4U 1608-522, 4U 1636-536, 4U 1702-429, 4U 1705-44, 4U 1728-34, KS 1731-260, Aql X-1, and XTE J2123-058, omitting 4U 1746-37 as explained in Sect. 3.1 (Galloway et al. 2008). While LWT bursts have associated S_z values of up to 2.8, SWT bursts all have $S_z \lesssim 2$.

⁴ Wijnands et al. (2002) found a pair of candidate bursts from MXB 1659-298 only ~ 50 s apart. The first flare, however, is relatively weak and lacks the cooling characteristic for Type I bursts. The second flare has been identified as γ -ray burst GRB 990419C (HEASARC IPNGRB catalog).

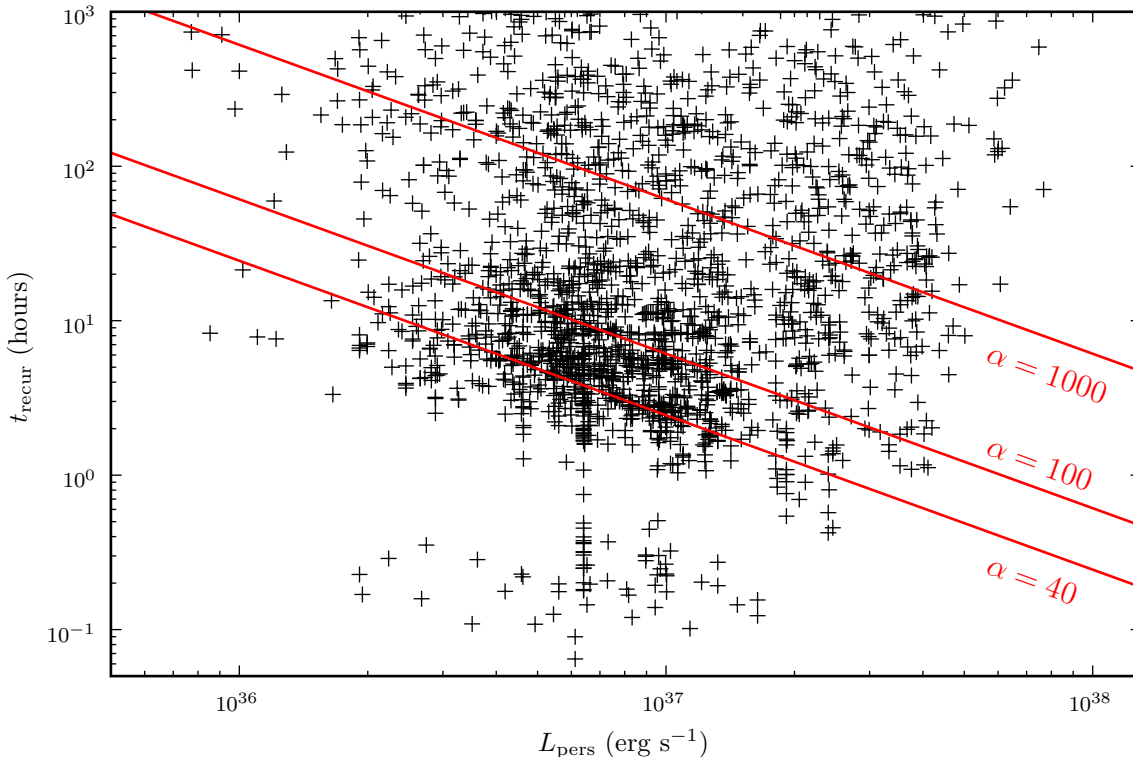


FIG. 5.— Observed recurrence time t_{recur} as a function of the persistent luminosity L_{pers} for 2415 bursts from 44 LMXBs. Due to the presence of data gaps, values of t_{recur} exceeding one hour are upper limits to the real recurrence time. We show bursts with $t_{\text{recur}} < 10^3$ hour. The lines represent constant values of the average α -parameter as indicated (see text). Note that the crosses indicate only the positions of the data points, not the uncertainties. The shortest recurrence time is 3.8 minutes.

Therefore, we find that SWT bursts are restricted to the so-called island state, while LWT bursts also occur in the ‘banana’ branch. A KS-test yields $P \simeq 10^{-3}$, confirming that the S_Z distributions for LWT and SWT bursts are different. Most of the SWT bursts from the frequent burster 4U 1636-53 occurred with $1.5 \lesssim S_Z \lesssim 2.0$. KS 1731-260 exhibits only a few LWT bursts in that range. This suggests that SWT bursts occur mainly in a small S_Z interval, and that the lack of SWT bursts from the latter source is caused by the low number of observed bursts in that range. Note that we observe SWT bursts with S_Z as low as 0.8, so the interval is not the same for all sources.

3.7. Frequency of short vs. long recurrence times

We consider 2415 bursts from hydrogen-accreting sources. 76 have a short recurrence time: the overall SWT fraction is $(3.1 \pm 0.4)\%$. The $1\text{-}\sigma$ uncertainty is derived from the Poisson uncertainties in the number of (SWT) bursts. As a function of persistent luminosity there is some variation in the SWT fraction, but there is no clear trend (Fig. 7). The weighted mean of the SWT fraction in the range of L_{pers} where SWT bursts are observed is $(2.3 \pm 0.3)\%$ for all hydrogen-rich accretors, $(13 \pm 4)\%$ for 4U 1636-536, $(16 \pm 4)\%$ for 2S 1742-294 and $(6 \pm 2)\%$ for EXO 0748-676.

We compare these fractions to *XMM-Newton* and *Chandra* observations of EXO 0748-676. In 2003 the *XMM-Newton* EPIC PN observed double and triple bursts from EXO 0748-676 with an SWT fraction of

$(32 \pm 7)\%$ (Boirin et al. 2007). Homan et al. (2003) find in *XMM-Newton* EPIC PN and MOS observations from 2000 and 2001 4 single and 4 double bursts, which results in an SWT fraction of $(33 \pm 19)\%$. *Chandra* ACIS-S observations from 2001 and 2003 exhibit 41 bursts with an SWT fraction of $(27 \pm 9)\%$ (see Appendix). The weighted mean of these rates is $(30 \pm 5)\%$. An important difference in the data of on the one hand *XMM-Newton* and *Chandra*, and on the other hand *RXTE* and *BeppoSAX*, is the frequent data gaps in observations of the latter observatories. From Monte Carlo simulations we found that data gaps reduce an SWT fraction of 30% to 20% (Sect. 3.3). This is significantly higher than the $(6 \pm 2)\%$ we obtain from MINBAR. We repeat the simulations for 4U 1636-536 and 2S 1742-294, using the mean SWT recurrence times from MINBAR: 16.2 min. and 20.5 min., respectively. The obtained SWT fractions, respectively 18% and 16%, are consistent within 1.3σ with the fractions from MINBAR.

The discrepancy for EXO 0748-676 may arise because of the fact that the WFCs are less sensitive to fainter bursts than the PCA or the instruments on *XMM-Newton* and *Chandra*. Taking only the PCA bursts into account, we find SWT fractions of $(11 \pm 6)\%$ for EXO 0748-676, $(13 \pm 4)\%$ for 4U 1636-53, and $(23 \pm 6)\%$ for 2S 1742-294, all of which are within 1.5σ from the fractions found from the Monte Carlo simulations.

Two frequent bursters exhibit no SWT bursts: KS 1731-26 and GS 1826-24. Combining the number of LWT bursts observed from these sources, we derive an

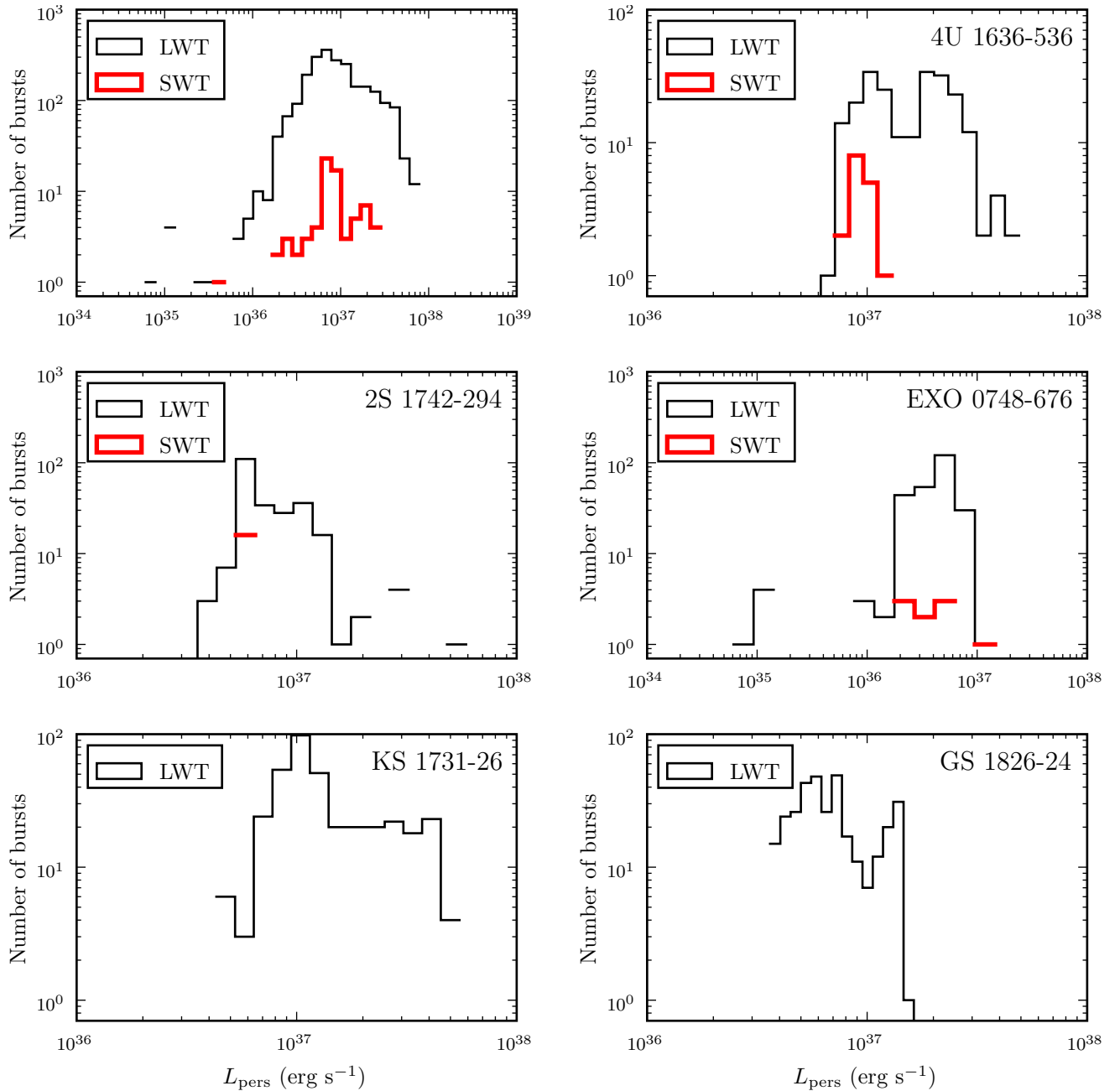


FIG. 6.— Histogram of bolometric persistent luminosity L_{pers} of LWT and SWT bursts, for all hydrogen-rich accretors (top-left) and for five individual sources. There is a dip in the distribution for all sources around $L_{\text{pers}} \simeq 1.7 \cdot 10^{37} \text{ erg s}^{-1}$. This is due to similar dips in the distributions of 4U 1636-53 and 2S 1742-294, as well as peaks in the distributions of KS 1731-26 and GS 1826-24 at slightly lower L_{pers} .

upper limit to the SWT fraction of 0.14%. This is over 20 times smaller than the SWT fraction we find for all hydrogen-accreting sources combined.

3.8. Temperature and energetics

From time-resolved spectral analysis of the bursts, we obtain the black-body temperature and the burst energetics. The peak temperature of the first bursts in multiple-burst events is on average higher than the peak temperature of the SWT bursts (Fig. 8). A KS test shows that the temperature distributions for single bursts and first bursts are not compatible ($P \simeq 10^{-12}$).

We compare the peak luminosity and the fluence of single bursts to those in multiple-burst events (Fig. 9,

Fig. 10). The SWT bursts have on average a lower peak luminosity and a lower fluence. The energetics of the first bursts does not follow the same distributions as the single bursts ($P \lesssim 10^{-2}$). By adding the fluence of all bursts in a multiple-burst event, we calculate the total event fluence (Fig. 11). Multiple-burst events are on average more energetic than single burst events, but do not have a higher fluence than the most energetic single bursts.

Summarizing, SWT bursts are on average weaker and cooler than LWT bursts, but the combined fluence in multiple-burst events is on average 8% higher than the fluence of single-burst events.

3.9. Decay time scale

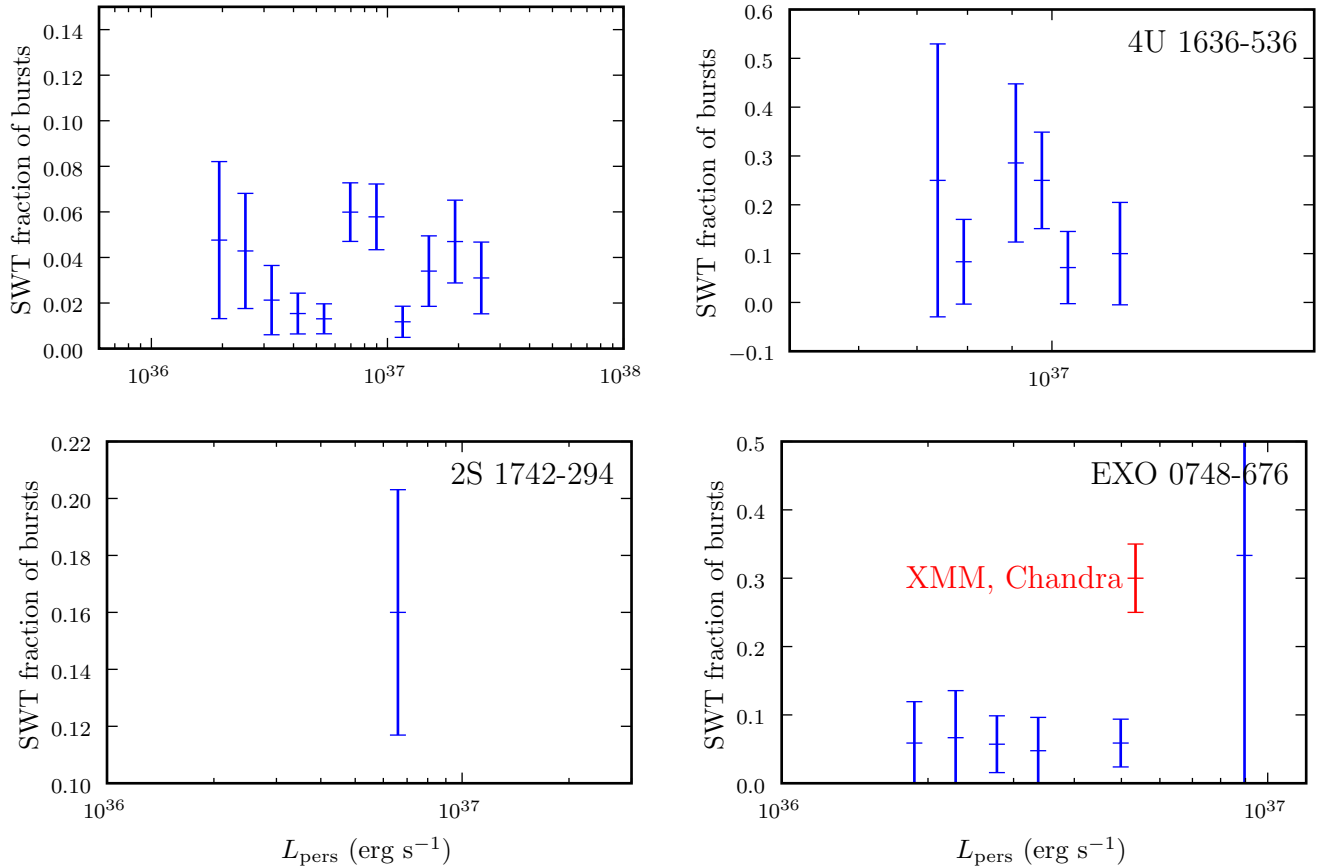


FIG. 7.— The fraction of bursts that have a short recurrence time as a function of the persistent luminosity L_{pers} , for all hydrogen-rich accretors (top-left) and for three individual sources. For each plot L_{pers} is divided into 30 logarithmically spaced bins, and for each bin the SWT fraction is calculated from the bursts in the corresponding plots in Fig. 6. For EXO 0748-676 one SWT burst is observed at higher L_{pers} , which results in a data point with large uncertainty.

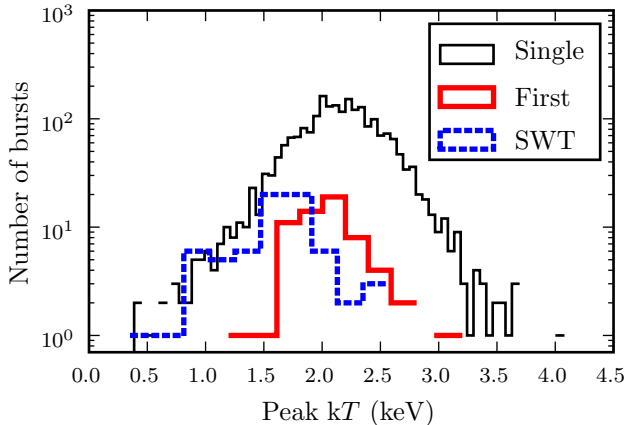


FIG. 8.— Histogram of peak black-body temperature of single bursts, the first bursts in multiple events, and the SWT bursts.

The two component exponential provides a good fit to many bursts. If the two-component decay does not provide a significantly better fit than the one-component, we use the latter. We compare the longest decay time scales of all bursts in Fig. 12. On average, the SWT bursts decay faster than the other bursts. KS tests show that all distributions are incompatible ($P \lesssim 10^{-2}$).

3.10. Neutron stars with SWT bursts spin fast

The spin frequency ν_{spin} of an accreting neutron star is measured in observations of accretion-powered pulsa-

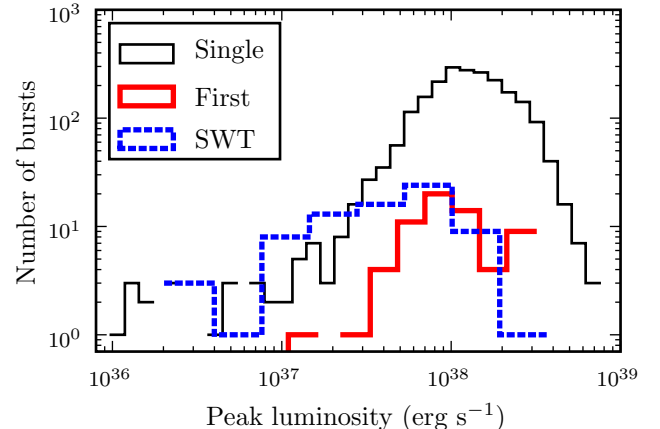


FIG. 9.— Histogram of bolometric peak luminosity of single bursts, the first bursts in multiple events, and the SWT bursts.

tions or burst oscillations. Both mechanisms are thought to arise from hotter and, hence, brighter spots on the surface rotating in and out of view. Currently ν_{spin} is known for 25 accreting neutron stars, 19 of which are bursters (e.g., Galloway 2008). Among them are 5 sources that exhibit SWT bursts (Table 1). They are concentrated towards the high-frequency part of the distribution for all bursting sources (Fig. 13). Since we only have five multiple-bursting sources with a known spin frequency, we cannot exclude that this bias is the result of the small sample.

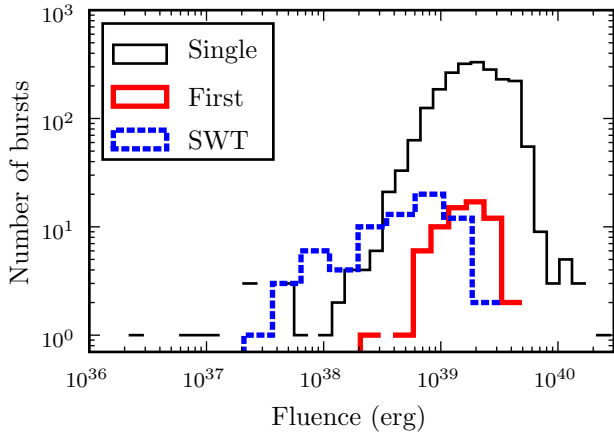


FIG. 10.— Histogram of bolometric fluence of single bursts, the first bursts in multiple events, and the SWT bursts.

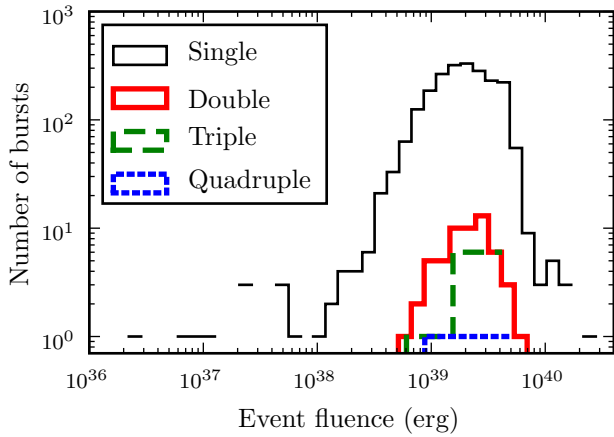


FIG. 11.— Histogram of the summed bolometric fluence of all bursts in the different multiple-burst events.

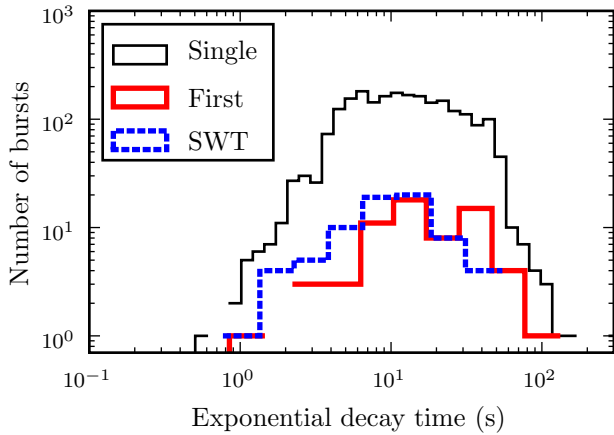


FIG. 12.— Histogram of the exponential decay time for single bursts of hydrogen-rich accretors, as well as the first and SWT bursts in multiple events.

There could be a selection effect: sources with a higher mass accretion rate accrete more angular momentum, causing them to spin up faster. Furthermore, their burst rate is higher, making it easier to detect a rare multiple-burst event. We check the MINBAR catalog for the number of bursts from these sources as a function of the spin frequency (Fig. 13). There is roughly an equal number

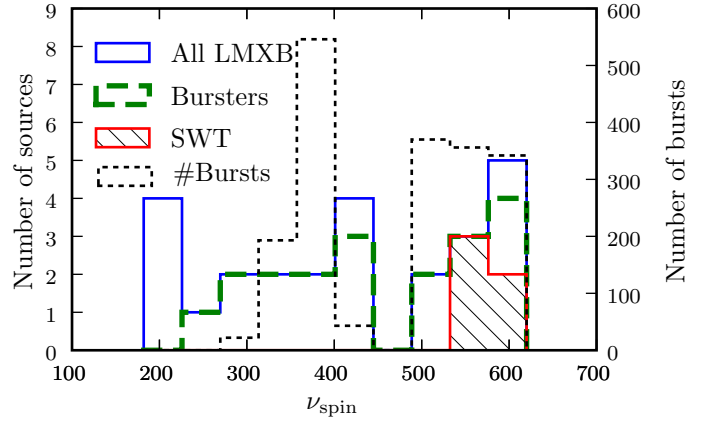


FIG. 13.— Histogram of the neutron star spin ν_{spin} determined from X-ray observations, for all LMXBs with known spin, for the known bursters and for the sources that exhibit multiple-bursts (Table 1). The latter are concentrated at the high end of the distribution of known spins. The dotted line indicates the number of bursts in the MINBAR catalog for the bursters in each bin (right-hand axis).

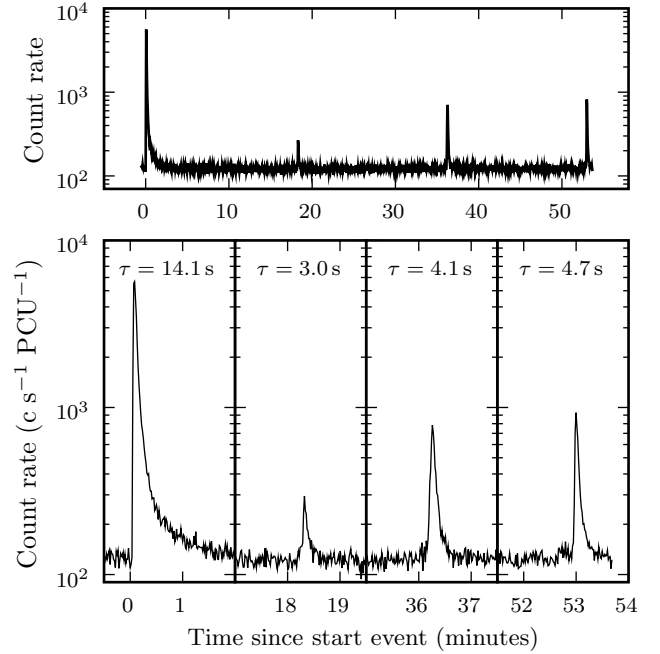


FIG. 14.— Quadruple burst from 4U 1636-53 as observed with the *RXTE* PCA on MJD 52286. Light curve at 2 s time resolution (*top*) and zoomed in on each burst at 1 s time resolution (*bottom*). For each burst we indicate the (longest) exponential decay time τ .

of bursts observed at higher and at lower ν_{spin} , so the selection effect is not present.

There are a few hydrogen-accreting sources of which we detected a large number of bursts, but no SWT bursts (Sect. 3.6). One of these sources, KS 1731-260, is known to have a large spin frequency of $\nu_{\text{spin}} = 524$ Hz (Smith et al. 1997).

3.11. Quadruple burst from 4U 1636-53

To illustrate the properties of LWT and SWT bursts, of which we have shown the distributions using a large number of bursts from the catalog, we consider the quadruple burst from 4U 1636-53 (Fig. 14). The four bursts

occurred within 54 minutes, and the time between the burst onsets is 18.2 min, 17.9 min, and 16.8 min, respectively. As indicated in Fig. 14, the first burst has by far the longest decay time τ . The first burst has a peak flux and fluence that is over seven times larger than any of the three SWT bursts. The peak black-body temperature (kT) of the four bursts is, respectively, (1.67 ± 0.02) keV, (1.06 ± 0.06) keV, (1.51 ± 0.06) keV, and (1.50 ± 0.04) keV: again the first burst has the highest value. The combined net burst fluence of the quadruple event is $(2.93 \pm 0.05) 10^{39}$ erg, which is 35% higher than the average fluence of single bursts from this source. and 27% higher than the fluence of the first burst from the quadruplet. This means that at least 27% of the available fuel did not burn in the initial burst.

4. DISCUSSION

We study the short recurrence time behavior in a large sample of bursts from multiple sources. We use a preliminary version of the MINBAR burst catalog, containing 3387 Type I X-ray bursts from 65 sources. 15 sources exhibit bursts with recurrence times less than one hour: SWT bursts. The short recurrence times do not allow for the accretion of the hydrogen and helium that is burned during the burst, which means that it must have been accreted before the previous burst. For example, the burst fluences from the quadruple event we observe from 4U 1636-53 indicate that at least 27% of the accreted fuel did not burn in the first burst. This is in contradiction with current one-dimensional multi-zone models, which predict that during a flash over 90% of the available fuel is burned (e.g., Woosley et al. 2004). The aim of this study is to provide a comprehensive observational assessment of the SWT behavior.

4.1. Temperature and energetics

We perform time resolved spectroscopy of the bursts, and find that SWT bursts are on average less bright and reach a lower black-body temperature at the peak than the LWT bursts. The fluence of SWT bursts is on average lower, but the combined bursts in a multiple-burst event are as energetic as the most energetic single bursts. This is in agreement with the *XMM-Newton* observations of EXO 0748-676 analyzed by Boirin et al. (2007). In contrast to that investigation, however, we find that the distributions of these quantities for single and for first bursts of multiple-burst events are not compatible according to Kolmogorov-Smirnov tests. It is possible that our improved statistics allows us to see a disparity that previously went unnoticed.

4.2. Multiple surface regions vs. multiple layers

Several ideas have been put forward to explain SWT bursts in an attempt to answer the two main questions: how to preserve fuel during a burst for the next burst, and how to reignite this fuel on a time scale of approximately ten minutes. Subsequent bursts with short recurrence time may take place in different regions of the neutron star surface. The accreted matter may be confined by a magnetic dipole field to the poles of the neutron star, or perhaps the burning front of a burst is stalled at the equator if the inflow of matter from the accretion disk is particularly strong there. This would provide an

explanation for double bursts, but the triple and quadruple bursts that we observe would require a more complicated configuration of the magnetic field. Furthermore, Boirin et al. (2007) find for EXO 0748-676 that there is no evidence for a difference in the X-ray emitting region during the different bursts of multiple-burst events. Also, they find indications that SWT bursts burn a fuel mixture with a lower hydrogen content, which would not be the case if different regions of pristine accreted material are burned. We, therefore, favor the scenario where SWT bursts take place in different layers on top of each other (Fujimoto et al. 1987). For this to work, the thermonuclear burning during the flash must be halted before the hydrogen and helium is depleted.

4.3. No SWT bursts from UCXBs

We observe no SWT bursts from any of the 16 (candidate) ultra-compact sources from which in total 229 bursts have been observed with the PCA and WFCs. For this reason we excluded these sources from our analyses. For the hydrogen-accreting sources we found a fraction of 3.1% of all bursts are SWT bursts. If we assume the same SWT fraction for the most frequently bursting confirmed UCXB, 4U 1820-303, we expect 1.7 SWT bursts out of the 54 bursts observed by the PCA and WFCs. The Poisson probability of detecting no SWT bursts when expecting 1.7, is 0.18. Taking into account the bursts from all confirmed and candidate UCXBs, we expect 7 SWT bursts, and the probability of a non-detection is less than 10^{-3} .

Based on its bursting behavior, 4U 1728-34 is a suspected UCXB (Galloway et al. 2008). If we include the 543 observed by the PCA and WFCs from this source, the expected number of SWT bursts is 23, and the probability of detecting none is 10^{-10} .

4.4. Thermonuclear burning processes

No SWT bursts are observed from UCXBs, but only from sources that are thought to accrete hydrogen-rich matter. This suggests that the nuclear burning processes involving hydrogen, i.e., the hot CNO cycle, the αp -process, and the rp -process, are important for creating SWT bursts. The rp -process is a series of proton captures and β -decays, that creates heavy isotopes with mass numbers up to approximately 100 (Schatz et al. 2001). In this reaction chain there might be a nuclear waiting point with the correct time scale to interrupt and reignite the thermonuclear burning, for example the time scale for spontaneous β -decay of an isotope. We find, however, a broad distribution of short recurrence times t_{recur} (Fig. 5), which argues against a single waiting point in the reaction chain (see also Boirin et al. 2007). Note that we do not detect SWT bursts from all hydrogen-rich accretors, the two frequent bursters KS 1731-26 and GS 1826-24 being the best examples. This means that merely accreting hydrogen is not enough to produce SWT bursts.

The decay profile of an X-ray burst is shaped by two processes. First there is radiative cooling on a thermal time scale. For normal bursts, which ignite at a typical column depth of $y \simeq 10^8$ g cm², this time scale is $\tau_{\text{therm}} \simeq 10$ s. A second process, that slows down the decay, is prolonged thermonuclear burning through

the *rp*-process, which lasts up to approximately 100 s (Schatz et al. 2001). For EXO 0748-676 Boirin et al. (2007) found SWT bursts to lack the second slower decay component, while the first bursts clearly exhibit a two-component exponential decay. We confirm that this holds true for the other sources with SWT bursts as well. This supports the conclusion by Boirin et al. (2007) that follow-up bursts must occur in a layer with a significantly reduced hydrogen content.

in 't Zand et al. (2009) found observations where the burst decay can be followed for several thousands of seconds. They explain the long tail as due to the cooling of a deeper layer below the bursting layer, that is heated by the burst. One of these long tails is detected for the first burst in a triple event of EXO 0748-676. The tail continues to decay uninterrupted while the second and third bursts occur. This is consistent with the idea that SWT bursts occur in a layer above the ignition depth where the first burst occurs. Taking into account that SWT bursts are less energetic, the deeper layer would not be heated substantially by the SWT bursts and continues to cool.

4.5. Mass accretion rate dependence

SWT bursts are observed over the entire range of mass accretion rates \dot{M} where LWT bursts are observed. For some individual sources, however, the SWT bursts occur in a smaller \dot{M} interval than LWT bursts. This is supported by the position in the color-color diagram where SWT bursts are observed (Sect. 3.6; Galloway et al. 2008). Other frequent bursters exhibit no SWT bursts at all, even though the ranges of \dot{M} we observe from sources with and without SWT bursts overlap. Because of the large uncertainty in converting flux to accretion rate, the precise overlap is uncertain.

At low accretion rates SWT recurrence times t_{recur} are mostly restricted to $3.8 \text{ min} \lesssim t_{\text{recur}} \lesssim 40 \text{ min}$. Above approximately $0.05 \dot{M}_{\text{Edd}}$, where the Eddington limited mass accretion rate \dot{M}_{Edd} corresponds to a persistent luminosity of $L_{\text{Edd}} = 2 \cdot 10^{38} \text{ erg s}^{-1}$ for hydrogen-accreting sources, recurrence times occur also in the range $40 \text{ min} \lesssim t_{\text{recur}} \lesssim 60 \text{ min}$. At $0.05 \dot{M}_{\text{Edd}}$ a transition between two burst regimes is predicted by Fujimoto et al. (1981) (see also Bildsten 1998). For lower accretion rates all accreted hydrogen burns in a stable manner, and the burst ignites in a hydrogen-poor layer. At higher rates there is no time to burn all hydrogen, and the burst ignites in a layer containing a substantial fraction of both hydrogen and helium. It may be that the latter regime allows for short recurrence times as long as an hour, while the former regime does not.

4.6. Rotation and mixing

The spin frequency ν_{spin} is not known for most accreting neutron stars, as it requires the observation of X-ray pulsations or burst oscillations (e.g., Galloway 2008). For five sources with short recurrence times ν_{spin} is known: all five are fast spinning neutron stars with $\nu_{\text{spin}} \gtrsim 500 \text{ Hz}$ (Table 1). The fast rotation could be required for the occurrence of multiple-burst events. It induces rotational instabilities, for example shear instabilities (e.g., Fujimoto 1988), and instabilities due to a rotationally

induced magnetic field (Spruit 2002), that mix the neutron star envelope on a time scale of approximately ten minutes (Piro & Bildsten 2007; Keek et al. 2009). If the thermonuclear burning during a flash is halted before it reaches higher layers, the hydrogen and helium in those layers will be mixed down. On a ten minute time scale it reaches the depth where temperature and density are sufficiently high to create the thermonuclear runaway for the next burst.

At accretion rates higher than $0.05 \dot{M}_{\text{Edd}}$, we find bursts with short recurrence times as long as an hour. We mentioned that this may be related to the transition to a different burst regime. The time scale for rotational mixing depends strongly on the thermal and compositional profile of the neutron star envelope (e.g., Heger et al. 2000 for the case of massive stars), which may vary for different burning regimes or even different bursts. This could provide an explanation for the spread in the observed recurrence times. Further theoretical study is necessary to better understand this.

The occurrence of multiple-burst events in sources with high rotation rates has consequences for the hypothesis that strong magnetic fields at the neutron star surface contain accreted matter at the poles. This would explain multiple bursts as caused by the burning of different magnetically-confined patches at the poles. The presence of a strong magnetic field, however, would allow for the transportation of angular momentum away from the neutron star, causing it to spin slower. The observations of short recurrence time bursts preferentially at high ν_{spin} seems in contradiction with this, which disfavors the magnetic-confinement scenario.

KS 1731-260 spins at a high frequency of 524 Hz, accreted hydrogen-rich material, and exhibited many bursts (369 in MINBAR). No short recurrence times were observed. Therefore, while a high rotation rate may support the occurrence of SWT bursts, it is not possible to discriminate between sources with and without SWT bursts based on this property alone. Possibly a combination of fast rotation and a mass accretion rate within a certain range (see previous section) are required for short recurrence times.

4.7. Frequency of SWT bursts

We investigate the SWT fraction: the number of bursts that have a short recurrence time with respect to the total number of observed bursts. We determine this fraction, at the persistent luminosities where SWT bursts are observed, for three frequent bursters with SWT bursts: EXO 0748-676, 4U 1636-53, and 2S 1742-294. *XMM-Newton* and *Chandra* observations of EXO 0748-676 find an SWT fraction of $(30 \pm 5)\%$. Our burst sample is obtained from *RXTE* PCA and *BeppoSAX* WFC observations, which contain data gaps due to Earth occultations and due to the South-Atlantic Anomaly. Monte-Carlo simulations show that the data gaps reduce an SWT fraction of 30% to 20%. An additional problem is the fact that the WFCs are less sensitive to fainter bursts than the PCA or the instruments on *XMM-Newton* and *Chandra*. Especially for EXO 0748-676 we find a much lower SWT fraction than from the *XMM* and *Chandra* observations. Taking only the PCA bursts into account, we find SWT fractions of $(11 \pm 6)\%$ for EXO 0748-676, $(13 \pm 4)\%$ for 4U 1636-53, and $(23 \pm 6)\%$ for 2S 1742-

294, all of which are within 1.5σ from the SWT fractions we obtain from Monte Carlo simulations, with an initial SWT fraction of 30%. Therefore, in the range of mass accretion rates where SWT bursts occur, approximately 30% of the bursts have a short recurrence time.

5. CONCLUSIONS

We studied thermonuclear bursts with short recurrence times (SWT) using a large catalog of bursts from multiple sources observed with the *RXTE* PCA and the *BepoSAX* WFCs. The short recurrence times are of insufficient duration to accrete the fuel that burns in an SWT burst. Bursts are seen to occur in events of up to four bursts: double, triple and quadruple bursts. We report the shortest recurrence time ever found: 3.8 minutes. We confirm the result of Boirin et al. (2007), that SWT bursts are on average less bright, cooler, and less energetic than LWT bursts. The decay profiles of SWT bursts lack the longer decay component from the *rp*-process, suggesting that SWT bursts take place in a hydrogen-depleted layer.

Some sources exhibit short recurrence times at all values of the mass accretion rate where normal bursts occur, while for others SWT bursts are limited to a smaller range of accretion rate. In this range the fraction of bursts with a short recurrence time is consistent with 30%. Two frequent bursters that likely accrete hydrogen-

rich matter do not show any SWT bursts.

Only the hydrogen-accreting neutron stars in our catalog exhibit SWT bursts. This suggests that the hydrogen-burning processes are responsible for the incomplete burning of the available hydrogen and helium during bursts. The mechanism for halting the burning is still unknown. It will require further theoretical modeling of hydrogen-accreting neutron star envelopes to resolve this issue.

As far as we know the spin of the sources with SWT bursts, they are all fast rotators. This indicates that rotational mixing can be responsible for ignition of follow-up bursts on a time scale of approximately 10 minutes (Piro & Bildsten 2007; Keek et al. 2009). The number of SWT sources with known spin is small. Measurements of the spin frequency for more sources and further model studies of rotational mixing will better constrain this reignition scenario.

LK is supported by the Joint Institute for Nuclear Astrophysics (JINA; grant PHY02-16783), a National Science Foundation Physics Frontier Center. AH acknowledges support from the DOE Program for Scientific Discovery through Advanced Computing (SciDAC; DE-FC02-09ER41618) and and by the US Department of Energy under grant DE-FG02-87ER40328.

REFERENCES

- Anders, E., & Ebihara, M. 1982, *Geochim. Cosmochim. Acta*, 46, 2363
- Aoki, T., et al. 1992, *PASJ*, 44, 641
- Belian, R. D., Conner, J. P., & Evans, W. D. 1976, *ApJ*, 206, L135
- Bildsten, L. 1998, in *NATO ASIC Proc. 515: The Many Faces of Neutron Stars.*, ed. R. Buccheri, J. van Paradijs, & A. Alpar, 419
- Boella, G., Butler, R. C., Perola, G. C., Piro, L., Scarsi, L., & Bleeker, J. A. M. 1997, *A&AS*, 122, 299
- Boirin, L., Keek, L., Méndez, M., Cumming, A., in't Zand, J. J. M., Cottam, J., Paerels, F., & Lewin, W. H. G. 2007, *A&A*, 465, 559
- Cornelisse, R., et al. 2003, *A&A*, 405, 1033
- Fender, R., Belloni, T., & Gallo, E. 2005, *Ap&SS*, 300, 1
- Fujimoto, M. Y. 1988, *A&A*, 198, 163
- Fujimoto, M. Y., Hanawa, T., & Miyaji, S. 1981, *ApJ*, 247, 267
- Fujimoto, M. Y., Sztajno, M., Lewin, W. H. G., & van Paradijs, J. 1987, *ApJ*, 319, 902
- Fushiki, I., & Lamb, D. Q. 1987, *ApJ*, 323, L55
- Galloway, D. 2008, in *American Institute of Physics Conference Series, Vol. 983, 40 Years of Pulsars: Millisecond Pulsars, Magnetars and More*, 510–518
- Galloway, D. K., Chakrabarty, D., Cumming, A., Kuulkers, E., Bildsten, L., & Rothschild, R. 2004a, in *American Institute of Physics Conference Series, Vol. 714, X-ray Timing 2003: Rossi and Beyond*, ed. P. Kaaret, F. K. Lamb, & J. H. Swank, 266–272
- Galloway, D. K., Cumming, A., Kuulkers, E., Bildsten, L., Chakrabarty, D., & Rothschild, R. E. 2004b, *ApJ*, 601, 466
- Galloway, D. K., Lin, J., Chakrabarty, D., & Hartman, J. M. 2009, *ArXiv e-prints*
- Galloway, D. K., Muno, M. P., Hartman, J. M., Psaltis, D., & Chakrabarty, D. 2008, *ApJS*, 179, 360
- Gold, T. 1968, *Nature*, 218, 731
- Gottwald, M., Haberl, F., Parmar, A. N., & White, N. E. 1986, *ApJ*, 308, 213
- . 1987a, *ApJ*, 323, 575
- Gottwald, M., Stella, L., White, N. E., & Barr, P. 1987b, *MNRAS*, 229, 395
- Grindlay, J., Gursky, H., Schnopper, H., Parsignault, D. R., Heise, J., Brinkman, A. C., & Schrijver, J. 1976, *ApJ*, 205, L127
- Gruber, D. E., Blanco, P. R., Heindl, W. A., Pelling, M. R., Rothschild, R. E., & Hink, P. L. 1996, *A&AS*, 120, C641+
- Hasinger, G., & van der Klis, M. 1989, *A&A*, 225, 79
- Heger, A., Cumming, A., Galloway, D. K., & Woosley, S. E. 2007, *ApJ*, 671, L141
- Heger, A., Langer, N., & Woosley, S. E. 2000, *ApJ*, 528, 368
- Homan, J., Wijnands, R., & van den Berg, M. 2003, *A&A*, 412, 799
- in 't Zand, J. J. M., Cumming, A., van der Sluys, M. V., Verbunt, F., & Pols, O. R. 2005, *A&A*, 441, 675
- in 't Zand, J. J. M., Jonker, P. G., & Markwardt, C. B. 2007, *A&A*, 465, 953
- in 't Zand, J. J. M., Keek, L., Cumming, A., Heger, A., Homan, J., & Méndez, M. 2009, *A&A*, 497, 469
- in 't Zand, J. J. M., Kuulkers, E., Verbunt, F., Heise, J., & Cornelisse, R. 2003, *A&A*, 411, L487
- in 't Zand, J. J. M., et al. 2004, *Nucl. Phys. Proc. Suppl.*, 132, 486
- Jager, R., et al. 1997, *A&AS*, 125, 557
- Jahoda, K., Markwardt, C. B., Radeva, Y., Rots, A. H., Stark, M. J., Swank, J. H., Strohmayer, T. E., & Zhang, W. 2006, *ApJS*, 163, 401
- Keek, L., in 't Zand, J. J. M., & Cumming, A. 2006, *A&A*, 455, 1031
- Keek, L., Langer, N., & in 't Zand, J. J. M. 2009, *A&A*, 502, 871
- Kuulkers, E., den Hartog, P. R., in 't Zand, J. J. M., Verbunt, F. W. M., Harris, W. E., & Cocchi, M. 2003, *A&A*, 399, 663
- Kuulkers, E., Homan, J., van der Klis, M., Lewin, W. H. G., & Méndez, M. 2002, *A&A*, 382, 947
- Lamb, D. Q., & Lamb, F. K. 1978, *ApJ*, 220, 291
- Lamb, F. K., Boutloukos, S., Van Wassenhove, S., Chamberlain, R. T., Lo, K. H., Clare, A., Yu, W., & Miller, M. C. 2009, *ApJ*, 706, 417
- Lattimer, J. M., & Prakash, M. 2007, *Phys. Rep.*, 442, 109
- Lewin, W. H. G., et al. 1976, *MNRAS*, 177, 83P
- Lewin, W. H. G., van Paradijs, J., & Taam, R. E. 1993, *Space Science Reviews*, 62, 223
- Linares, M., et al. 2009, *The Astronomer's Telegram*, 1979, 1
- Liu, Q. Z., van Paradijs, J., & van den Heuvel, E. P. J. 2007, *A&A*, 469, 807
- Maraschi, L., & Cavaliere, A. 1977, in *Highlights in Astronomy*, ed. E. A. Müller, Vol. 4 (Reidel, Dordrecht), 127

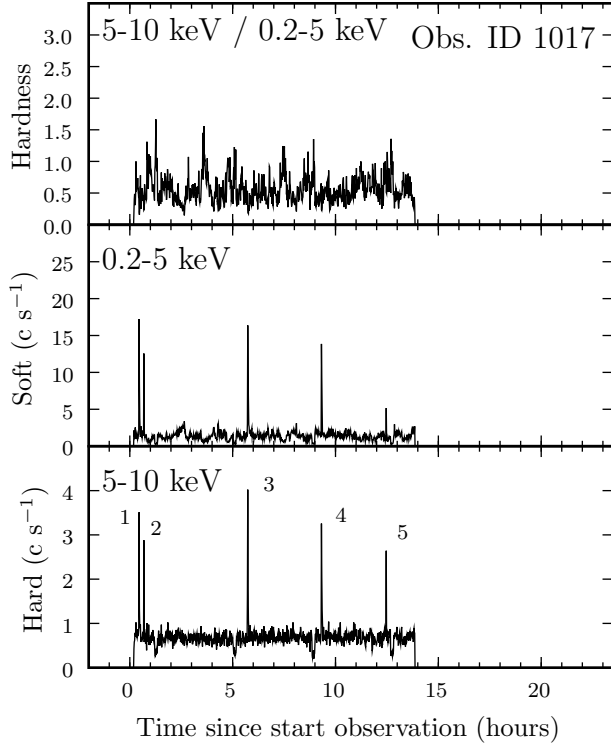


FIG. 15.— *Chandra* light curves of EXO 0748-676 as observed in 2001 and 2003. We show the hard and soft energy bands as well as the hardness ratio. The observation id is indicated. In the hard band we number the bursts. Figure continues on next page.

Melatos, A., & Payne, D. J. B. 2005, *ApJ*, 623, 1044
Morrison, R., & McCammon, D. 1983, *ApJ*, 270, 119
Muno, M. P., Chakrabarty, D., Galloway, D. K., & Psaltis, D. 2002, *ApJ*, 580, 1048
Murakami, T., et al. 1980, *PASJ*, 32, 543
Piro, A. L., & Bildsten, L. 2007, *ApJ*, 663, 1252
Schatz, H., et al. 2001, *Physical Review Letters*, 86, 3471
Smith, D. A., Morgan, E. H., & Bradt, H. 1997, *ApJ*, 479, L137+
Spruit, H. C. 2002, *A&A*, 381, 923
Strohmayer, T., & Bildsten, L. 2006, *New views of thermonuclear bursts (Compact stellar X-ray sources)*, 113–156
Strohmayer, T. E., Zhang, W., Swank, J. H., White, N. E., & Lapidus, I. 1998, *ApJ*, 498, L135+
Taam, R. E., Woosley, S. E., Weaver, T. A., & Lamb, D. Q. 1993, *ApJ*, 413, 324

van Paradijs, J., Penninx, W., & Lewin, W. H. G. 1988, *MNRAS*, 233, 437
Wallace, R. K., & Woosley, S. E. 1981, *ApJS*, 45, 389
Wijnands, R., Muno, M. P., Miller, J. M., Franco, L. M., Strohmayer, T., Galloway, D., & Chakrabarty, D. 2002, *ApJ*, 566, 1060
Wijnands, R., Strohmayer, T., & Franco, L. M. 2001, *ApJ*, 549, L71
Woosley, S. E., et al. 2004, *ApJS*, 151, 75
Woosley, S. E., & Taam, R. E. 1976, *Nature*, 263, 101
Zhang, W., Jahoda, K., Kelley, R. L., Strohmayer, T. E., Swank, J. H., & Zhang, S. N. 1998, *ApJ*, 495, L9+

APPENDIX

CHANDRA OBSERVATIONS OF EXO 0748-676

Chandra ACIS-S observations with High-Energy Transmission Grating (HETG) in 2001 and 2003 of EXO 0748-676. We use the level 2 event files prepared by the *Chandra* Data Archive and select events from a circle centered on the source and two bands overlapping the signal from the gratings. Using the CIAO software package (version 4.1), we extract light curves in the 0.2 – 5 keV and 5 – 10 keV energy bands at 60 s time resolution, and calculate the hardness ratio by taking the ratio of the count rates in the hard and soft bands (Fig. 15). The light curves are similar to the *XMM-Newton* observations performed in 2001 and 2003. Eclipses are present at the binary period of 3.8 h. Especially in the data from 2003, dipping is present in the soft band. We, therefore, use the hard band to locate bursts. We find a total of 41 bursts; 11 have a short recurrence time. The burst events are divided into 20 singles, 9 doubles, and 1 triple. The SWT fraction is $(27 \pm 9)\%$. Note that burst 22 of observation 4573 appears anomalously long. This is caused by a raised detector background level during a few hundred seconds after the burst, combined with the bin size of 60 s we used for the figure.

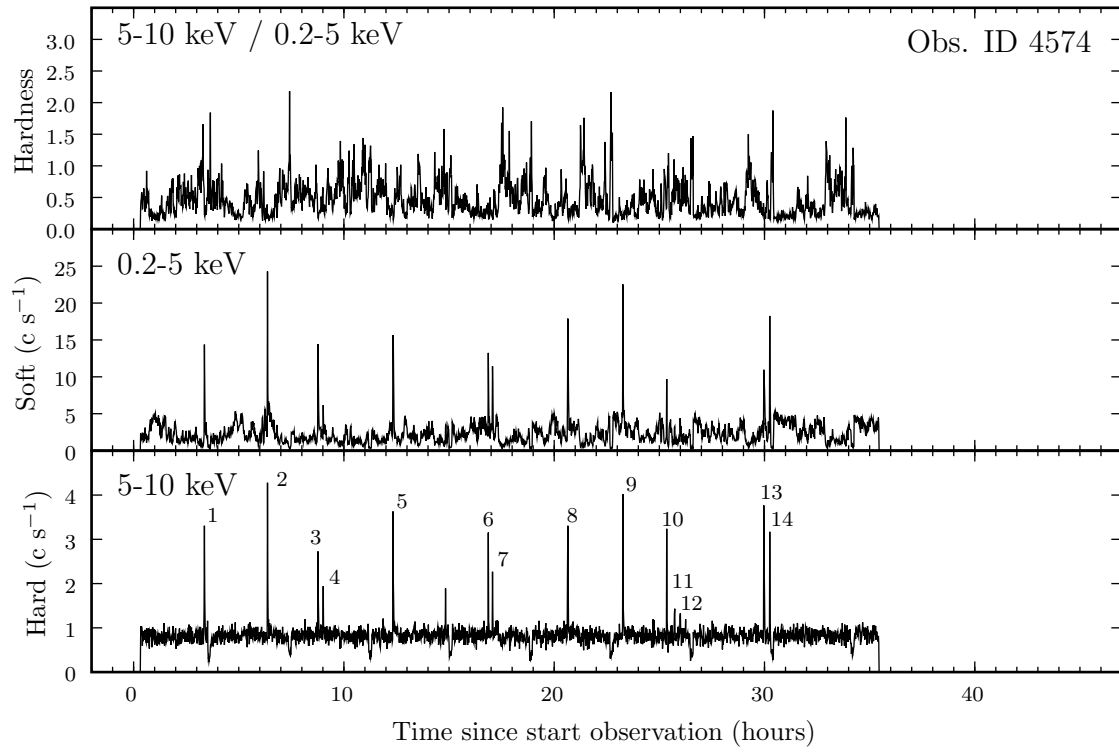
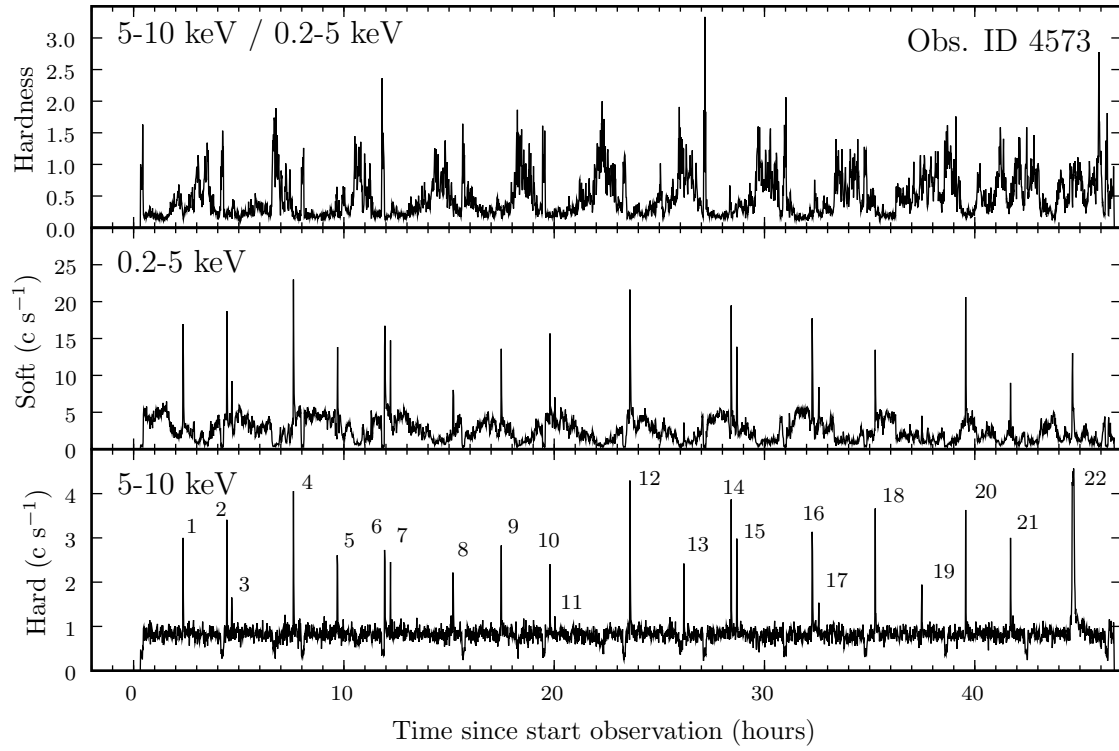


FIG. 15 CONTINUED.